International Journal of Robotics and Control Systems
Vol. 5, No. 1, 2025, pp. 570-584
ISSN 2775-2658
http://pubs2.ascee.org/index.php/ijrcs

Modeling the Structural Dynamics of Carbon Fiber Composites for Robotic Systems Under Sinusoidal Load

Raheem Al-Sabur [a,1,*], Yahya Muhammed Ameen [a,2], Hassanein I. Khalaf [a,3], Akshansh Mishra [b,4], Abdel-Nasser Sharkawy [c,5]

[a] Mechanical Engineering Department, University of Basrah, Basrah 61004, Iraq
[b] School of Industrial and Information Engineering, Politecnico di Milano, Milan 20133, Italy
[c] Mechanical Engineering Department, Faculty of Engineering, South Valley University, Qena 83523, Egypt
[1] raheem.musawel@uobasrah.edu.iq; [2] yahya.ameen@uobasrah.edu.iq; [3] hassanein.khalaf@uobasrah.edu.iq;
[4] akshansh.mishra@mail.polimi.it; [5] eng.abdelnassersharkawy@gmail.com
* Corresponding Author

ARTICLE INFO

Article history
Received October 31, 2024
Revised December 21, 2024
Accepted January 24, 2025

Keywords
Modeling;
Free Vibration Modeling;
Composite Shells;
Bending Analysis;
PPS Composite;
Robotic System

ABSTRACT

The demand for robotic systems employing composite materials is steadily improving due to their high bending stiffness, favorable strength-to-weight ratio, and durability under dynamic loading. It is still challenging to guarantee dynamic stability and precise frequency response in composite robotic components. This study addresses these issues by conducting a simulation-based 3D bending analysis and frequency response modeling of carbon/epoxy and carbon/PPS composites under sinusoidal loading. The remarkable mechanical and thermal properties of carbon/epoxy and carbon/PPS composites, such as their high specific strength, stiffness, and excellent fatigue resistance, align well with the requirements of robotic systems. The model comparison involved analyzing three-dimensional bending stresses, displacements, and free vibration dynamics for both materials under a sinusoidal load applied to their inner surfaces. The sinusoidal load was selected to simulate periodic dynamic forces commonly encountered in robotic applications, such as oscillating arms, vibrating components, and cyclic loading during operation. The thick shell (S=4) of axial length (L=4S) and circumferential span (α=45°) comprises cross-ply laminate [90°/0°/90°] with supported boundary conditions. The transverse displacement of the carbon PPS composite cylindrical shell was 0.719 nm, which was lower than that of the carbon epoxy composite (0.746 nm). The same behavior was observed for the stress values. Conversely, the PPS composite cylindrical shell yielded a higher natural frequency. The obtained eigenvalues indicated a similar behavior when comparing the shape modes with a relative increase in their values in the carbon PPS composite.

1. Introduction

Engineering materials that incorporate several different constituents of matter with radically differing properties are called composite materials. The use of composite materials has completely changed how we construct things. The unique features of a composite material are determined by the volumetric ratio, the arrangement of its constituent parts, and the specific characteristics of each

member [1], [2]. Although the beginnings of the use of composite materials date back to ancient times, the beginning of the use of modern composite materials in the form known today dates back to the 1930s [3], [4]. Composite materials offer many advantages over traditional materials, including higher strength, stiffness, and durability while being lightweight and resistant to corrosion and other environmental factors [5], [6]. Composite materials have many uses, from everyday products to high-tech applications. Due to their lighter weight and more fuel-efficient nature, composites are most used in the aerospace and transportation industries. They are also widely used in consumer products and the construction industry [7], [8].

Because composite materials are lightweight and durable under dynamic loads, they can offer outstanding strength and performance, which is driving growing demand for robotic systems based on them [9], [10]. Dealing with the structural stability of lightweight gives composites an edge over conventional materials. In the field of robotic control, design considerations for the overall structure and grippers, as well as cameras, have become attractive elements for the use of composite materials, especially carbon-reinforced composites [11], [12]. Therefore, the use of composite materials, especially those based on carbon fibers, has received great attention in the fields of robotics [13]-[15]. Three categories divide the main applications of composite materials in robotics: lightweight structures, precision components, and energy efficiency [16], [17]. In the lightweight structures category, robotic arms, exoskeletons, drones, and UAVS are the primary subdivisions [18]. At the same time, grapplers, medical robots, and manufacturing robots for high speed are typical examples of the use of composite materials as precision components in robots [19], [20]. Conversely, within the Efficiency category, typical applications of composite materials include autonomous vehicles, underwater robots, and battery housings [21], [22]. Fig. 1 summarizes the main types and subcategories of composite materials used in robotic components.

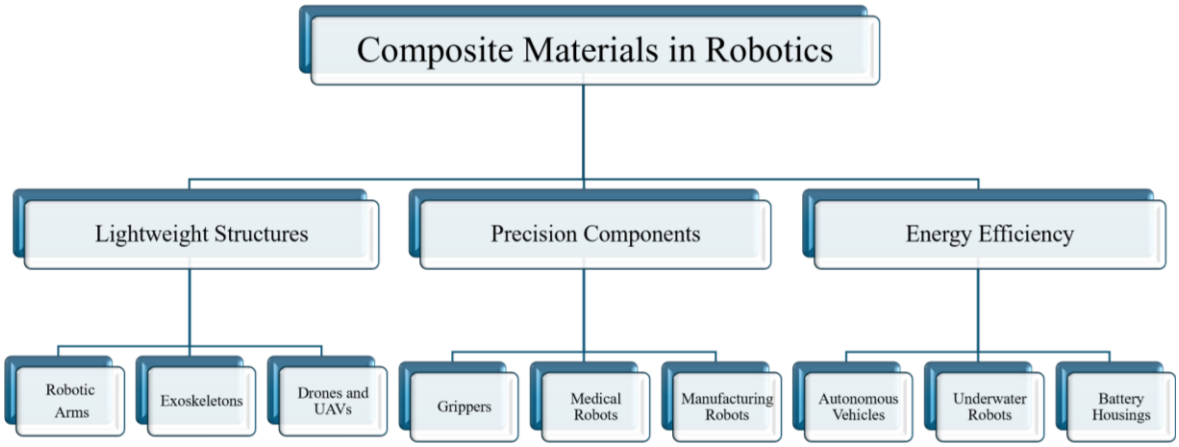

Fig. 1. Main applications of composite materials in robotic fields

Carbon/epoxy composites offer high specific strength and stiffness, making them ideal for structural components in robotic systems that require lightweight and high mechanical performance. In contrast, carbon/PPS composites provide thermal stability and chemical resistance, making them suitable for high temperatures and harsh environments [23], [24]. When high performance and lightweight are the primary goals, composite materials made from reinforcing fiber, such as carbon fiber, with a resin matrix system, such as epoxy, are ideal [25], [26]. The epoxy bonds the materials, reducing buckling and increasing load transfer between the fibers [27], [28]. The fibers' high strength is due to their strong carbon-carbon molecular bonds [29]. Polyphenylene sulfide (PPS) is a high-performance thermoplastic polymer with exceptional heat, chemical, and electricity resistance. It is substantial, lightweight, and durable enough to withstand high temperatures without losing its properties [30], [31]. Their dimensional stability and good mechanical properties characterize PPS tubes, plates, and rods. In recent years, PPS has emerged as a successful low-cost alternative in applications where metal use is too heavy and design-limiting [32], [33].

Several studies were done to analyze the static and dynamic of laminated composite spherical shells applied to sinusoidal mechanical/thermal loads with supported boundary conditions. Ghugal et al. [34] investigated a trigonometric shear and normal deformation theory based on trigonometric functions in the parameter space. The theory takes into account both normal strain and transverse shear. Chen et al. [35] suggested a mesh-free First Shear Order Theory (FSDT) method based on the 3D continuous shell theory and the moving-least squares approximation to examine how arbitrary laminated composite shells and spatial structures move freely. The method's originality lies in the resulting mesh-free model's generalized geometric and kinematic representations, which are more readily applicable to intricate laminated shell geometries.

Meskini et al. [36] investigated the free vibrational dynamic analysis of adhesive joins between two laminated composite shells that were round, cylindrical, and conical, taking into account different boundary conditions. Their numerical results show that the structure with the adhesive layer had a higher non-dimensional frequency as the cone angle of the conical shell and the ratio of overlap length to shell length went up. Melaibari et al. [37] created a mathematical continuum model to look into the free vibration response of cross-ply carbon nanotube-reinforced composite laminated nanoplates and nanoshells, taking into account effects on the microstructure and the length scale. The analysis accounted for various shell geometries, including sheet (indefinite radii), spherical, cylindrical, hyperbolic-paraboloid, and elliptical-paraboloid. Kim et al. [38] examined the free vibration dynamic behavior of laminated composite spherical shells with varying thicknesses using the Haar wavelet discretization method (HWDM) as a numerical solution methodology. The first-order shear deformation theory (FSDT) provided a theoretical framework. Parmar et al. [39] used finite element modeling to demonstrate how composite and sandwich spherical shells respond to bending and vibration. ABAQUS modeled the shell as a three-dimensional deformable solid part, using mixed modeling techniques to model composites. Ferriera et al. [40] established a novel method for creating higher-order finite elements by incorporating progressive damage into the formulation. Carrera's universal formulation (CUF) serves as the foundation for the strategy, and Abaqus's FORTRAN UEL (User Element) subroutine implements the damage model. CDM is a continuum damage mechanics technique. The significant findings demonstrated that the applied UEL is accurate and quick enough to forecast successive failure occurrences and in-plane damage mechanisms for composite laminates subjected to bending loads. Wu et al. [41] provided theoretical and computational methods to examine the free vibration of orthogonally stiffened cylindrical shells. The total energy of the stiffened cylindrical shells was also deduced using the K'arman-Donnell shell theory. Cylindrical shells are often used as structural components in the aerospace industry due to their excellent load-carrying capability per unit weight. However, cutouts might drastically lower this capacity for carrying loads, particularly if cylindrical shells buckle under axial compression. It's critical to accurately forecast this value because the buckling load is frequently a vital design element [42].

Regarding the carbon/PPS composite materials and exploring these composites' properties, several studies were concluded. Chen et al. [43] investigated the household and aerospace applications of PPS/carbon composites and analyzed the anticipated major challenges. They concluded that PPS/carbon composites have the potential to enhance structural integrity and tribological and mechanical properties. Stoeffler et al. [44] explored the possibility of using specific percentages of recycled carbon fibers to form carbon-polyphenylene sulfide (PPS) composites. They found that the mechanical properties of the resulting composites were encouraging and very close to those obtained from using virgin carbon fibers. Furthermore, the addition of recycled materials did not affect the thermal stability, and the resulting polymer matrix exhibited a uniform distribution of fibers. Won et al. [45] explored the possibility of electroplating composites made of PPS and carbon fiber-reinforced composites by monitoring the interfacial shear strength. They concluded that the strong interphase in the interfacial region was the main reason for the PPS matrix's failure and fracture, and the maximum stress achieved was around 5 MPa. Zhang et al. [46] study the ability to produce a composite material consisting of a specific ratio of carbon fiber and PPS using condensation polymerization. The scanning electron microscopy (SEM) results showed improved macro-mechanical properties. Durmaz and Aytac [47] used injection molding and melt blending methods at different loading levels on carbon

fiber-reinforced and PPS composites and discovered that adding certain materials, such as Joncryl, can improve the strain and tensile strength values at fracture levels and improve the adhesion between the components of the resulting composite material. Kang et al. [48] investigated the possibility of using induction-heating molding to manufacture carbon fiber and PPS composite materials. They found that the tensile strength is flexible enough to reach above 2 GPa along 0° while it decreases significantly along 90°, not exceeding 46 MPa. They concluded that the proposed method can substantially save time and cost, which means facilitating material. This study looks at three main ways that carbon/epoxy and carbon/PPS composites move and bend: bending stresses, displacements, and free vibration dynamics under sinusoidal loading.

Previous literature indicates that, despite numerous studies integrating carbon fiber and PPS as composite materials, further research is necessary for 3D bending analysis and natural frequency evaluation. The primary purpose of this study is to look at the bending stresses, displacements, and free vibration dynamics of carbon/epoxy and carbon/PPS composites when they are loaded in a sinusoidal way. The study aims to provide insights into the structural and dynamic performance of these materials, specifically under conditions relevant to robotic systems. This study tries to provide a deep understanding of the structural dynamics of composite materials which is essential for their effective integration into robotic applications, especially under dynamic loads. The study will examine the stress distribution for both types of composite materials, utilizing 3D Von Mises stress and flexural stresses in tension and compression scenarios. Additionally, it will incorporate free vibration modeling analysis for eigenvalue, frequency (cycles/time), and generalized mass, all of which will be dependent on the shape modes.

2. Theoretical Model

Mechanical and structural engineers commonly use the sinusoidal load to model the behavior of materials under cyclic loading conditions. It can be used to study the response of materials and structures to fatigue loading, vibration, and other types of dynamic loads. The load can be visualized as a sinusoidal wave traveling through the material or structure as described in Eq. (1) [49].

$$p = p_0 cos\left(\pi \frac{z}{L}\right) cos\left(\pi \frac{\theta}{\alpha}\right) \tag{1}$$

Where p is the load or pressure applied to a material or structure, p_o is the amplitude of the load, z is the axial coordinate, measured along the length of the material or structure, L is the length of the material or structure, θ is the azimuthal coordinate, measured in the transverse direction around the circumference of the material or structure, α is the angular period of the load in the θ-direction. The stress is not homogeneous throughout the material because the wave's amplitude changes with the axial coordinate (z) and the azimuthal coordinate (θ). When the cosine terms in the equation have a value of 1, the load is at its highest; when they have a value of -1, the load is at its minimum. By altering the value of po, the load's amplitude can be changed. The load has a period of L in the axial direction and α in the azimuthal direction. In many studies, the load transfer at the interfaces between constituent parts or neighbouring layers has been modelled using the linear spring-layer model. In the case of a laminated cylindrical panel, as depicted in Fig. 2.

The corresponding model is summarized in Eq. (2)-(4) which describe the radial, azimuthal, and axial stresses and shear stresses in a cylindrical coordinate system at a specific radial distance $r = r_k$ from the center of a cylindrical structure or material [49].

$$\sigma_r{}^{(k+1)} = \sigma_r{}^{(k)} = \frac{\left[u_r{}^{(k+1)} - u_r{}^{(k)}\right]}{R_r{}^{(k)}} \tag{2}$$

$$\tau_{r\theta}{}^{(k+1)} = \tau_{r\theta}{}^{(k)} = \frac{\left[u_\theta{}^{(k+1)} - u_\theta{}^{(k)}\right]}{R_\theta{}^{(k)}} \tag{3}$$

$$\tau_{rz}{}^{(k+1)} = \tau_{rz}{}^{(k)} = \frac{\left[u_z{}^{(k+1)} - u_z{}^{(k)}\right]}{R_z{}^{(k)}} \quad (4)$$

Where $\sigma_r{}^{(k)}, \tau_{r\theta}{}^{(k)}\ and\ \tau_{rz}{}^{(k)}$ are the subjected radial normal stress, radial-azimuthal shear stress, radial-axial shear stress in the k_{th} layer and $R_i{}^{(k)}$ $(i = r, \theta, z)$ are the compliance constant of the interface between the k_{th} and $(k+1)_{th}$ layer. The subscript k indicates the iteration number, and the superscript (k+1) indicates the updated value of the variable at the next iteration. Equations (2)-(4) are derived using the linear spring-layer assumption, ensuring realistic load transfer across the interfaces. They were implemented in the simulation to evaluate stress distribution under sinusoidal loading. The equations use the displacement components ur, uθ, and uz, which represent the radial, azimuthal, and axial displacements, respectively, and the radii of curvature Rr, Rθ, and Rz, which represent the radii of curvature in the radial, azimuthal, and axial directions, respectively. The compliance constants describe the interface stiffness in the radial, circumferential, and longitudinal directions, respectively. The material properties and thickness of the adhesive or interfacial layer determine these constants. The model enables accurate simulation of interfacial interactions, ensuring realistic load distribution.

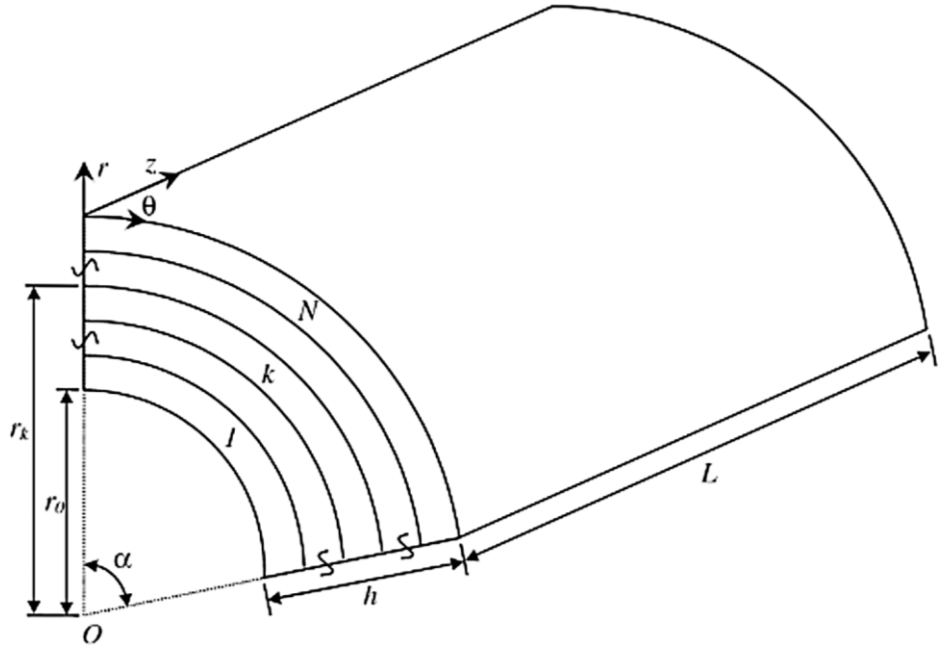

Fig. 2. Cylindrical coordinates and the geometry of a laminated cylindrical panel [50]

3. Cylindrical Shell Modeling Simulation

The process of creating a laminated cylindrical shell in Abaqus involved several steps. First, a new model was created, and the working directory was set. Then, a 3D deformable solid part was created. The process entails creating cylindrical coordinates, defining the material's mechanical properties, creating a section, assigning it to the body parts, setting up the material's orientation, creating a static analysis step, selecting the load module, defining the boundary condition, creating nodes, and meshing. A sinusoidal load is created with the mechanical load as a pressure. Focusing on the inner surface provides insights into how such loads influence stress and displacement distributions, which are critical for evaluating structural integrity. At the inner surface, give the expression for the sinusoidal load with respect to the coordinate system, where R, Th and Z are the axes, as shown in Fig. 3. The expression is $cos\left(\pi\frac{z}{16}\right)cos\left(\pi\frac{\theta}{4}\right)$, while for the analysis of free vibration, no load is applied. A quadratic type of 3D stress element is defined, and finally, the part is meshed. Boundary conditions involved fixed supports along [specific edges], and the mesh size was optimized through a sensitivity analysis to ensure result accuracy and computational efficiency [51].

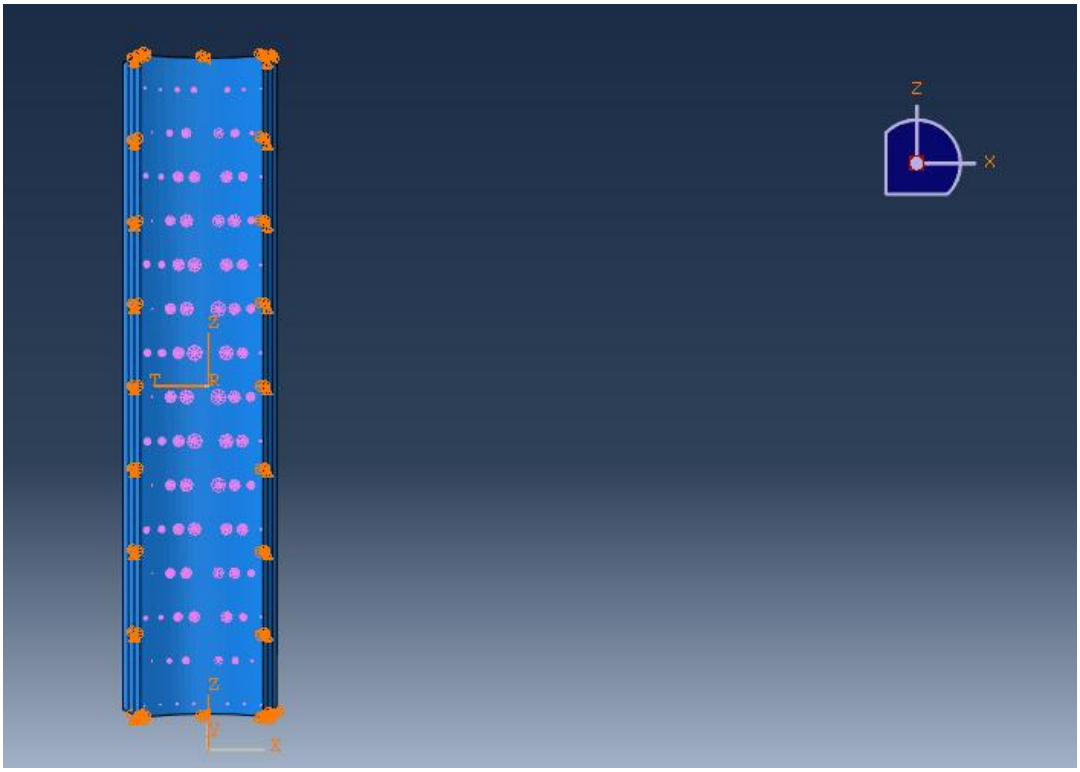

Fig. 3. Subjection of the sinusoidal load on the inner surface of the composite panel

The simply supported boundary condition used is following:

$$\sigma_z = u_\theta = u_r = 0, \quad at\ z = 0, L \tag{5}$$

$$\sigma_\theta = u_z = u_r = 0, \quad at\ \theta = 0, \alpha \tag{6}$$

The mechanical properties of Carbon Epoxy and Carbon PPS were presented in Table 1.

Table 1. Mechanical property of carbon epoxy and carbon PPS composites

Properties	Symbol	Carbon Epoxy	Carbon PPS
Elastic Modulus (GPa)	E1	172.5	51.08
	E2	6.9	41.34
	E3	6.9	41.34
Poisson's ratio	Nu12	0.25	0.03
	Nu13	0.25	0.03
	Nu23	0.25	0.03
Shear Modulus (GPa)	G12	3.45	4.12
	G13	3.45	3.5
	G23	1.38	3.5

The theoretical and simulation models assume idealized material behaviour and homogeneity, which may not fully reflect real-world conditions. These simplifications were necessary for the analysis, and the results should be viewed as foundational, with the potential for more complex modelling in future work. These notices are the main limitations of using this study.

4. Results and Discussion

Composite cylindrical shells are crucial in the robotics industry due to their exceptional strength-to-weight ratio, durability, and adaptability. The selected properties make them suitable for

applications such as robotic arms, where high performance and lightweight design are essential. The availability of composite materials in such components can enhance efficiency and develop robotic systems. Analyzing composite materials' behaviour under dynamic loads is highly relevant to advancing robotic technology. This section will discuss the 3D static and dynamic examination of composite cylindrical shells made of carbon epoxy and carbon /polyphenylene sulfide (PPS). Firstly, the stress distribution analysis of the carbon epoxy and carbon PPS laminates will be investigated, and then the free vibration analysis of composite cylindrical shells for both laminates will be investigated.

4.1. Stress Distribution in Composite Cylindrical Shells

The three axes in 3D Abaqus analysis show the orientation angles used to describe the ply orientations in the laminate, which is the carbon epoxy laminate and for carbon/PPS laminate. The 1-axis corresponds to the angle between the fiber direction of the first ply and the reference axis (usually the global x-axis). The 2-axis corresponds to the angle between the fiber direction of the first ply and the direction perpendicular to the reference axis and the 1-axis in the plane of the laminate. The 3-axis corresponds to the angle between the 1-axis and 2-axis in the direction perpendicular to the laminate. Understanding the trends of the axes in complex materials exposed to significant movement provides a deeper understanding of the fibre's direction, properties, and areas of weakness. The 1-axis typically aligns with the fibre direction, offering the highest strength and stiffness, while the 2-axis and 3-axis correspond to transverse directions, which are less stiff and weaker.

The stress distribution was examined based on von Mises stresses under loading conditions. The von Mises stress is computed using a formal equation based on the normal stresses and the shear stresses. The von Mises stress provides a scalar value that enables direct comparison to the material's yield strength, indicating whether the composite shell remains within the elastic deformation range. Stress values were calculated at critical regions of the composite shells under sinusoidal loading using the simulation output from ABAQUS. The stress distribution was investigated when the maximum von Mises stress was applied. This approach ensures the analysis accurately reflects the structural integrity of the composite shells under operational conditions.

Fig. 3 illustrates the increments at 7.0, the step time at 1.0, the deformed Var=U, and the deformation scale factor at 1.000 nm for the 3-axes. The orientation of the carbon epoxy laminate plies in the shells was obtained from the visualization module as shown in Fig. 4 a. The piles exhibit proper orientation. In composite materials such as carbon epoxy, the orientation of the fibers within the ply is of great importance because it is a decisive factor in determining the strength and stiffness of the material and even affects most of its mechanical properties [52], [53]. So, piles exhibit proper orientation, encouraging prediction of the resulting mechanical properties. Fig. 4 b shows the orientation of the plies of carbon PPS laminates in the shells obtained from the visualization module. As in epoxy carbon laminates, the plies are adequately oriented in carbon PPS laminates. This means that the resulting mechanical properties will meet expectations and can contribute to the design of engineering structures and other applications.

Fig. 5 a shows the nature of the Von Mises stress mesh effect on carbon epoxy laminate. The Von Mises stress is homogeneously elliptical along the carbon epoxy laminate, being small at all edges and growing steadily until it reaches maximum values at the center of the laminate [54]. The stress in the center is more evenly distributed, resulting in a higher concentration of von Mises stress. Moreover, under internal pressure, the material near the inner surface (closer to the center) tends to experience higher stress than the outer surface. This behavior is consistent with what Avcu et al. [55] discovered when testing pressure composite tanks. Regarding the carbon/PPS laminate, the Von Mises stress behavior was similar to that of carbon/epoxy laminate in distribution. Still, the maximum stresses at the center of the laminate were greater in the case of carbon/PPS, as shown in Fig. 5 b. This increase can be attributed to PPS being generally less stiff and less intense than epoxy resins, leading to higher localized stresses. The carbon/PPS laminate might deform more, which explains the relatively higher von Mises stress than the carbon/epoxy laminate. Furthermore, epoxy typically forms a stronger bond with carbon fibers than PPS, leading to better load transfer and greater effectiveness in reducing stress concentration [56].

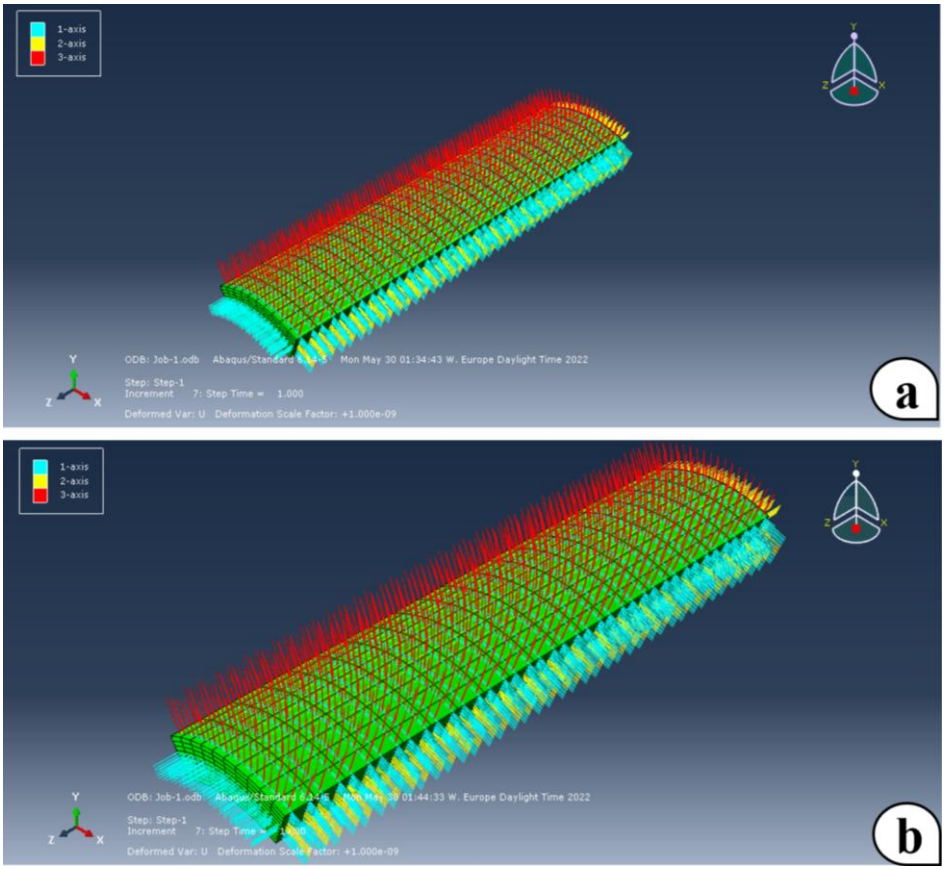

Fig. 4. Orientation of plies in a) carbon epoxy laminate b) carbon PPS laminates

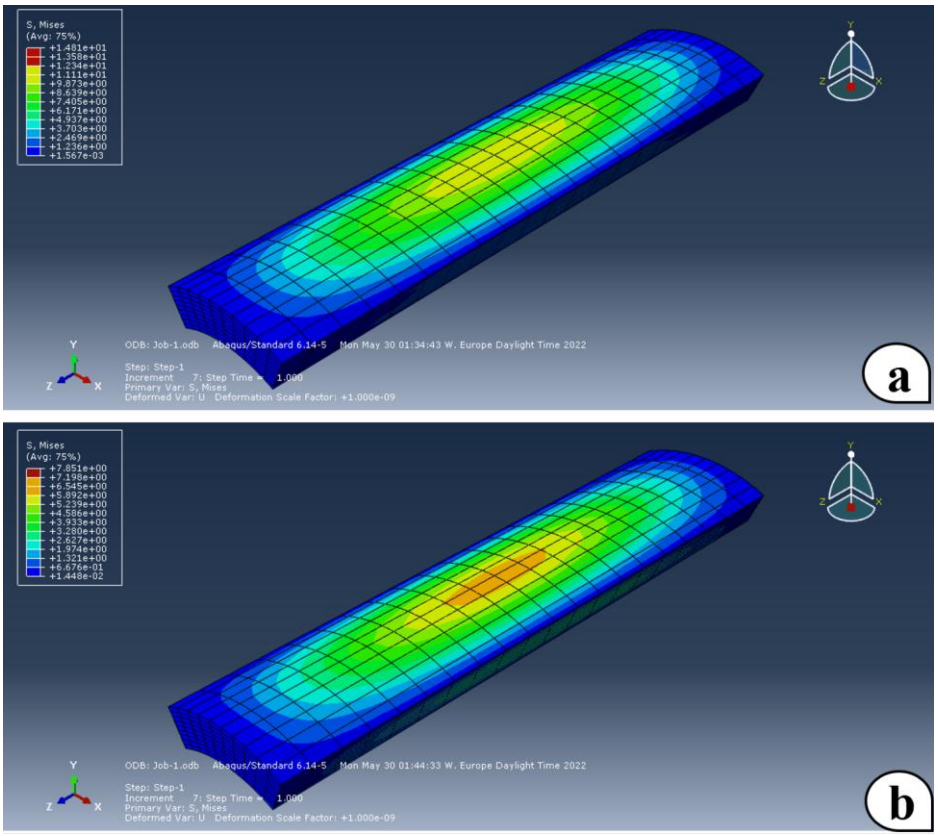

Fig. 5. Von mises stress mesh effect in a) carbon epoxy laminate b) carbon PPS laminates

The u_1 is the transverse displacement, and w' is the non-dimensionalized value of u_1, obtained from Eq. (3). For carbon epoxy laminates, the u_1 and w′ were 0.746 nm and 5.03, respectively, while for the carbon/PPS laminates the values were 0.719 nm and 1.44, respectively. The transverse displacement u_1 for carbon/epoxy laminates is slightly higher than that for carbon/PPS laminates, which means that under the same conditions, the transverse displacement is slightly higher for carbon/epoxy laminates, which suggests that the two materials are not stiff enough or don't respond well to load. The non-dimensionalized displacement w′ is much more significant for carbon/epoxy than for carbon/PPS, which makes the relative difference in displacement behavior even bigger. This could be because the materials have different properties, like modulus of elasticity, or they are made of different layers. σ_z is calculated at the middle section of inner and outer surfaces where stress values are high. σ_z is also non-dimensionalized to the σ_1' as per Eq. (4). σ_θ is also calculated at the middle section of inner and outer surfaces and is further normalized to σ_2' given by the Eq. (5). The transverse stress i.e., $\sigma_{r\theta}$ is calculated at the middle of the edge of the cylindrical shell and is further normalized to σ_3'

Table 2 provides the bending stress values for a carbon epoxy laminate under transverse loading. These values indicate the maximum and minimum stress experienced by the carbon epoxy laminate under transverse loading. The negative values of σ_z and σ_θ indicate compressive stresses, while the positive values indicate tensile stresses. The range of values indicates that the laminate's maximum tensile stress is 11.170 MPa, less than the allowable stress for carbon epoxy laminates. However, the maximum compressive stress experienced by the laminate is -15.539 MPa, which is more than the allowable stress. Therefore, the laminate may experience failure due to compressive stresses.

Note that these stress values, obtained under specific loading and boundary conditions, may not apply to all situations. When designing and selecting materials for a particular application, designers and engineers must consider these values and other factors, such as safety, fatigue, and environmental effects.

It is evident from the values of u1 and w' and the results of Table 2 that the carbon epoxy experiences more displacement than the carbon PPS composite cylindrical shell and that it also experiences higher stresses than the carbon PPS material. Moreover, Table 2 provides key stress values, with maximum stresses indicating critical points where material failure is most likely, while minimum stresses reflect regions of lower strain. These variations affected the structural integrity of the composite materials under typical dynamic loads, especially in robotic applications.

Table 2. Bending stresses for carbon epoxy and carbon /PPS laminates

Stresses	Compression	Tension	Compression	Tension
σ_z	-0.455	0.239	-0.487	0.904
σ_1'	-0.289	0.149	-0.3041	0.565
σ_θ	-15.539	11.1707	-8.584	6.669
σ_2'	-9.7121	6.981	-5.365	4.168
$\sigma_{r\theta}$	-0.94	1.09	-1.208	1.493
σ_3'	-2.35	2.726	-3.019	3.732

4.2. Free Vibration Modeling Analysis in Composite Cylindrical Shells

This section aims to find the composite shell's lowest natural frequency and visualize the mode shapes. Laminated composites typically produce lower natural frequencies, which can also significantly enhance the resonant phenomenon [57]. Therefore, the study of the lowest natural frequency in laminated materials is gaining importance due to the steady increase in engineering applications of these materials. The natural frequencies in this study revealed the effect of the sinusoidal load on both carbon epoxy and carbon/PPS composite shells. Each natural frequency corresponds to a specific mode shape (1, 2, and 3), which describes the pattern of deformation the structure undergoes during vibration. The eigenvalue is a scalar that relates stiffness and mass matrices. Usually, the smallest eigenvalue corresponds to the lowest natural frequency, while the highest values correspond to higher vibration modes. This can be observed in Table 3 for carbon epoxy

and Carbon PPS cylindrical shells; whereas the mode changes upwards, the Eigenvalues increase, accompanied by an increase in the frequency values.

Fig. 6 graphically shows the relationship between the mode shapes and related natural frequencies for the two composites under study. It is important to note that for all cases, the value of composite modal damping was = 0.

Mode shapes are typically visual representations of how different parts of a structure move relative to each other during vibration [58]. In the eigenvalue problem, eigenvectors mathematically represent them. Fig. 7 and Fig. 8, which depict the changes in mode shapes (1, 2, and 3) for carbon epoxy and carbon/PPS composite shells, clearly demonstrate the significant changes between mode 1 and mode 2 and between mode 2 and mode 3 for both cases. In the case of the carbon epoxy composite shell, there was a 300% increase in the eigenvalue between mode 1 and mode 2, and another increase of about 92% occurred when transitioning between mode 2 and mode 3. In the case of the carbon/PPS composite shell, the increase was comparable to that of the carbon epoxy composite between modes 1 and 2, but it was not as significant as the increase between modes 2 and 3, as it did not surpass 63%.

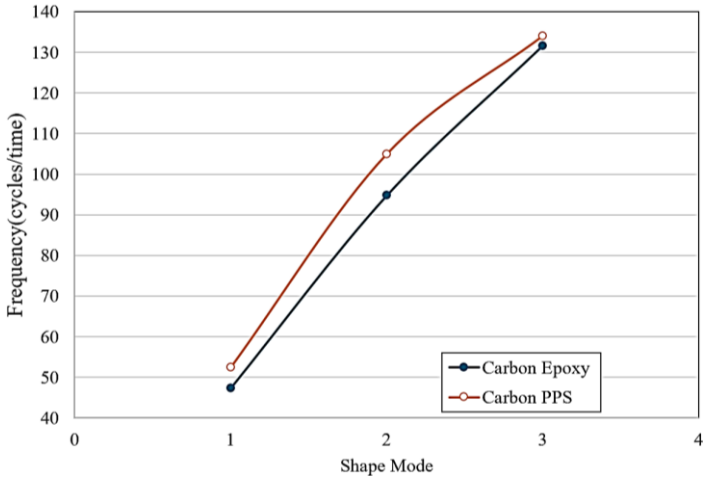

Fig. 6. Variation of the natural frequency modes for carbon epoxy and carbon PPS

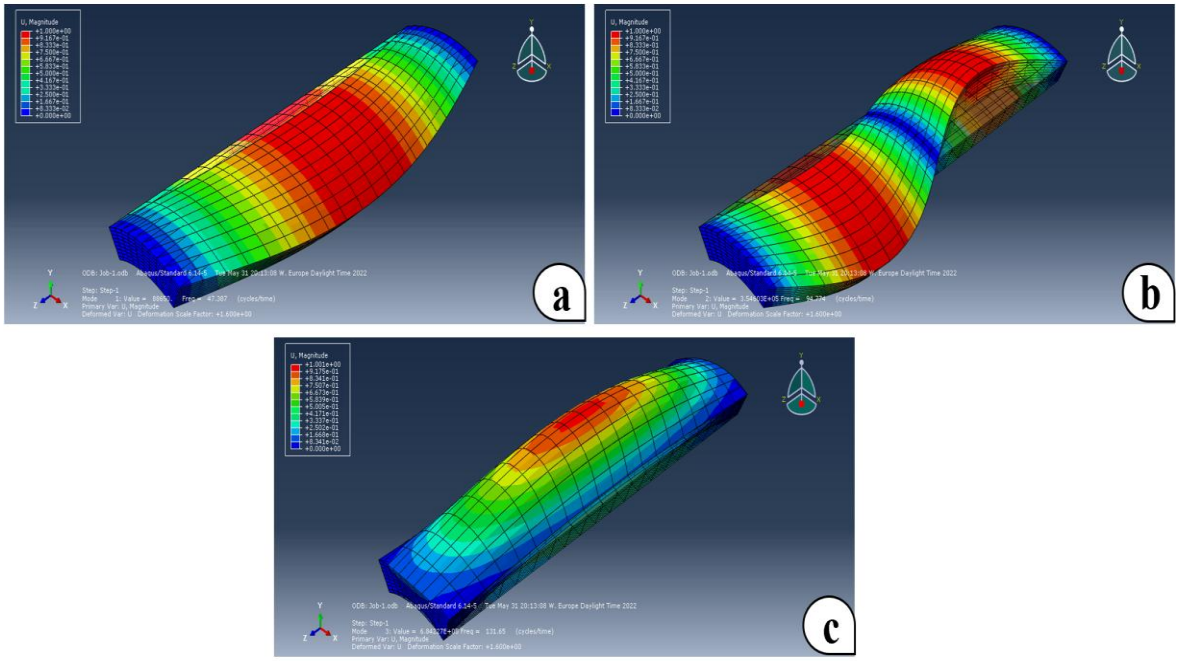

Fig. 7. Shapes of carbon epoxy cylindrical shell for a) mode 1, b) mode 2, c) mode 3

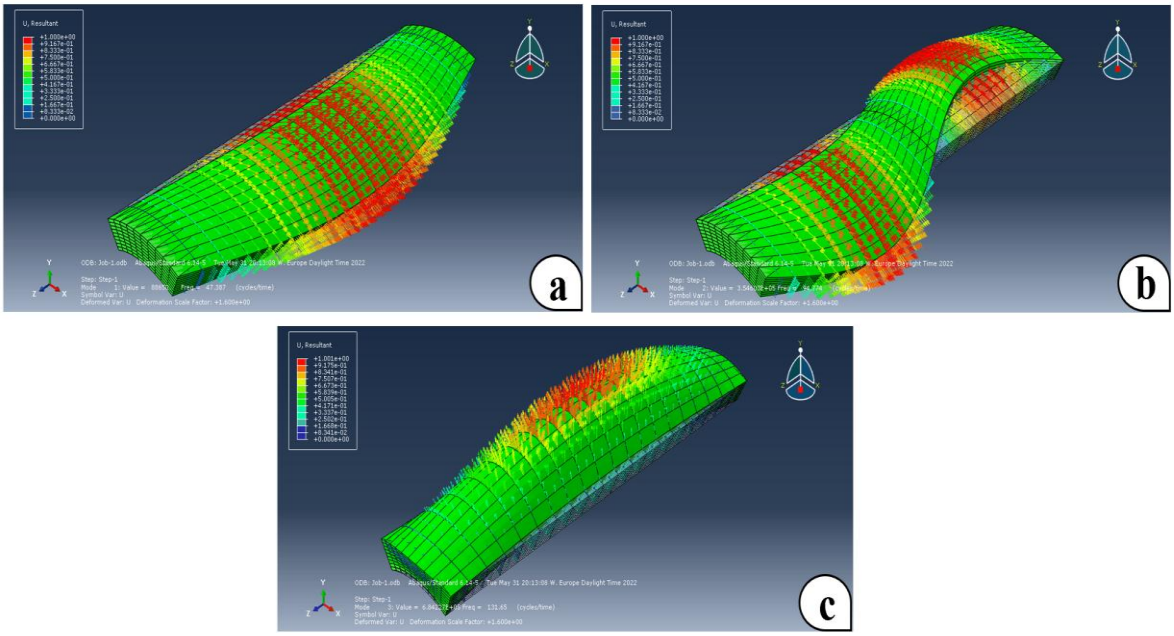

Fig. 8. Shapes of carbon/PPS cylindrical shell for a) mode 1, b) mode 2, c) mode 3

Table 3. Free vibrational analysis of carbon epoxy and carbon /PPS composite shell

Mode	Carbon Epoxy			Carbon PPS		
	1	2	3	1	2	3
Eigenvalue	88650	3.55E+05	6.84E+05	1.09E+05	4.35E+05	7.09E+05
Frequency (cycles/time)	47.387	94.774	131.65	52.493	104.99	134.05
Generalized Mass	33614	33613	21288	32717	32716	21973

5. Conclusion

The customizable properties of composite shells related to transverse displacement, natural frequency, and dynamic behavior can be tailored to stiffness and vibration damping. This understanding can enable designers to optimize robotic systems for precision and reliability in various applications. The recent study found that the carbon epoxy composite cylindrical shell had higher stress values than the carbon PPS composite cylindrical shell for the same magnitude of the applied sinusoidal load. The main conclusion of this study can be summarized as follows: The transverse displacement of the carbon PPS composite cylindrical shell was 0.719 nm, which was lower than that of the carbon epoxy composite (0.746 nm). The same behavior was observed for stress values. The magnitude of the carbon epoxy composite's lowest natural frequency is smaller than that of the carbon PPS composite cylindrical shell, which means that the Carbon PPS composite cylindrical shell outperforms the Carbon Epoxy composite cylindrical shell in terms of stability and fatigue resistance. Moreover, the mechanical and physical properties of composites are desirable, and the dynamic behavior of cylindrical shells is greatly affected by vibration mode shapes and boundary conditions. These parameters are essential and advantageous in the design stage of these composites and the study of structural health monitoring during operation. In addition, natural frequencies depend on the component's mass and stiffness in structural analysis. Higher mode frequency corresponds to stiffer components in either direction. In structural analysis, lower frequencies typically result in a component's displacement or deflection being higher, which causes the component to sustain more fatigue damage. Another consideration is whether the natural frequency (which may be high) is close to any stimulation frequency, in which case the component will suffer more fatigue damage.

Future studies could explore more composite materials, such as hybrid composites and bio-based polymers, to assess their performance under dynamic loading. Moreover, incorporating thermal and

environmental effects, fatigue analysis, and optimization techniques could further enhance the applicability of the findings.

Author Contribution: All authors contributed equally to the main contributor to this paper. All authors read and approved the final paper.

Funding: This research received no external funding.

Conflicts of Interest: The authors declare no conflict of interest.

References

[1] R. Al-Sabur, A. Kubit, H. Khalaf, W. Jurczak, A. Dzierwa, and M. Korzeniowski, "Analysis of Surface Texture and Roughness in Composites Stiffening Ribs Formed by SPIF Process," *Materials*, vol. 16, no. 7, p. 2901, 2023, https://doi.org/10.3390/ma16072901.

[2] Z. S. Toor, "Space Applications of Composite Materials," *Journal of Space Technology*, vol. 8, no. 1, pp. 65-70, 2018, https://www.ist.edu.pk/downloads/jst/previous-issues/july-2018/09.-space-applications-of-composite-materials1.pdf.

[3] A. Czapla, M. Ganesapillai, and J. Drewnowski, "Composite as a material of the future in the era of green deal implementation strategies," *Processes*, vol. 9, no. 12, p. 2238, 2021, https://doi.org/10.3390/pr9122238.

[4] S. Singh, M. Uddin, and C. Prakash, "Introduction, history, and origin of composite materials," *Fabrication and Machining of Advanced Materials and Composites: Opportunities and Challenges*, 2022, https://doi.org/10.1201/9781003327370-1.

[5] B. V. Ramnath, K. Alagarraja, and C. Elanchezhian, "Review on Sandwich Composite and their Applications," *Materialstoday: Proceedings*, vol. 16, pp. 859–864, 2019, https://doi.org/10.1016/j.matpr.2019.05.169.

[6] A. Kubit, R. Al-Sabur, A. Gradzik, K. Ochał, J. Slota, and M. Korzeniowski, "Investigating Residual Stresses in Metal-Plastic Composites Stiffening Ribs Formed Using the Single Point Incremental Forming Method," *Materials*, vol. 15, no. 22, p. 8252, 2022, https://doi.org/10.3390/ma15228252.

[7] M. Norkhairunnisa, T. C. Hua, S. M. Sapuan, and R. A. Ilyas, "Evolution of Aerospace Composite Materials," *Advanced Composites in Aerospace Engineering Applications*, pp. 367–385, 2022, https://doi.org/10.1007/978-3-030-88192-4_18.

[8] H. I. Khalaf and R. Al-Sabur, "Friction Stir Techniques Exploring Fracture and Fatigue Behavior in Hybrid Composite Joints," *Utilizing Friction Stir Techniques for Composite Hybridization*, pp. 108–134, 2024, https://doi.org/10.4018/979-8-3693-3993-0.ch007.

[9] I. M. Daniel, "Yield and failure criteria for composite materials under static and dynamic loading," *Progress in Aerospace Sciences*, vol. 81, pp. 18-25, 2016, https://doi.org/10.1016/j.paerosci.2015.11.003.

[10] L. Jing, K. Li, H. Yang, and P. Y. Chen, "Recent advances in integration of 2D materials with soft matter for multifunctional robotic materials," *Materials Horizons*, vol. 7, no. 1, pp. 54-70, 2020, https://doi.org/10.1039/C9MH01139K.

[11] J. Che, J. Kim, H. Lee, and S. Chang, "Application of carbon/epoxy composites to robot console structure for high stiffness with lightweight," *Composite Structures*, vol. 300, p. 116121, 2022, https://doi.org/10.1016/j.compstruct.2022.116121.

[12] A. Djavadifar, J. B. Graham-Knight, M. Körber, P. Lasserre, and H. Najjaran, "Automated visual detection of geometrical defects in composite manufacturing processes using deep convolutional neural networks," *Journal of Intelligent Manufacturing*, vol. 33, no. 8, pp. 2257–2275, 2022, https://doi.org/10.1007/s10845-021-01776-1.

[13] L. J. Zhang, Y. R. Zhao, and H. F. Xiang, "Research of a kind of new intelligent robot hand material," *Advanced Materials Research*, vol. 510, pp. 698-703, 2012, https://doi.org/10.4028/www.scientific.net/AMR.510.698.

[14] P. Duraisamy, R. Kumar Sidharthan, and M. Nagarajan Santhanakrishnan, "Design, Modeling, and Control of Biomimetic Fish Robot: A Review," *Journal of Bionic Engineering*, vol. 16, pp. 967-993, 2019, https://doi.org/10.1007/s42235-019-0111-7.

[15] A. Kebritchi, S. Havashinezhadian and M. Rostami, "Design and Experimental Development of Hexapod Robot with Fiberglass-Fibercarbon Composite Legs," *2018 6th RSI International Conference on Robotics and Mechatronics (IcRoM)*, pp. 439-444, 2018, https://doi.org/10.1109/ICRoM.2018.8657521.

[16] Z. Zhu *et al*., "High precision and efficiency robotic milling of complex parts: Challenges, approaches and trends," *Chinese Journal of Aeronautics*, vol. 35, no. 2, pp. 22-46, 2022, https://doi.org/10.1016/j.cja.2020.12.030.

[17] M. Soori, B. Arezoo, and R. Dastres, "Optimization of energy consumption in industrial robots, a review," *Cognitive Robotics*, vol. 3, pp. 142-157, 2023, https://doi.org/10.1016/j.cogr.2023.05.003.

[18] S. Siengchin, "A review on lightweight materials for defence applications: Present and future developments," *Defence Technology*, vol. 24, pp. 1-17, 2023, https://doi.org/10.1016/j.dt.2023.02.025.

[19] T. Kopp, M. Baumgartner, S. Kinkel, "Success factors for introducing industrial human-robot interaction in practice: an empirically driven framework," *The International Journal of Advanced Manufacturing Technology*, vol. 112, pp. 685-704, 2021, https://doi.org/10.1007/s00170-020-06398-0.

[20] F. Xu, F. Meng, Q. Jiang, and G. Peng, "Grappling claws for a robot to climb rough wall surfaces: Mechanical design, grasping algorithm, and experiments," *Robotics and Autonomous Systems*, vol. 128, p. 103501, 2020, https://doi.org/10.1016/j.robot.2020.103501.

[21] J. Wang, Z. Wu, H. Dong, M. Tan and J. Yu, "Development and Control of Underwater Gliding Robots: A Review," *IEEE/CAA Journal of Automatica Sinica*, vol. 9, no. 9, pp. 1543-1560, 2022, https://doi.org/10.1109/JAS.2022.105671.

[22] J. Boaretto *et al*., "Biomimetics and composite materials toward efficient mobility: A review," *Journal of Composites Science*, vol. 5, no. 1, p. 22, 2021, https://doi.org/10.3390/jcs5010022.

[23] D. G. Lee, C. S. Lee, H. G. Lee, H. Y. Hwang, and J. W. Kim, "Novel applications of composite structures to robots, machine tools and automobiles," *Composite Structures*, vol. 66, no. 1–4, pp. 17-39, 2004, https://doi.org/10.1016/j.compstruct.2004.04.044.

[24] Emy A. Sharif *et al*., "Physical, Thermal and Mechanical Properties of Carbon Fibre/Polyphenylene Sulfide (CF/PPS) Composite at Different Tool Temperatures Fabricated by Hot Press," *Journal of Advanced Research in Applied Mechanics*, vol. 117, no. 1, pp. 190–203, 2024, https://doi.org/10.37934/aram.117.1.190203.

[25] Z. Xu *et al*., "Additive manufacturing of two-phase lightweight, stiff and high damping carbon fiber reinforced polymer microlattices," *Additive Manufacturing*, vol. 32, p. 101106, 2020, https://doi.org/10.1016/j.addma.2020.101106.

[26] C. Zheng, F. Duan, and S. Liang, "Manufacturing and mechanical performance of novel epoxy resin matrix carbon fiber reinforced damping composites," *Composite Structures*, vol. 256, p. 113099, 2021, https://doi.org/10.1016/j.compstruct.2020.113099.

[27] J. Qureshi, "A Review of Fibre Reinforced Polymer Structures," *Fibers*, vol. 10, no. 3, p. 27, 2022, https://doi.org/10.3390/fib10030027.

[28] Ö. Özbek, "Axial and lateral buckling analysis of kevlar/epoxy fiber-reinforced composite laminates incorporating silica nanoparticles," *Polymer Composites*, vol. 42, no. 3, pp. 1109-1122, 2021, https://doi.org/10.1002/pc.25886.

[29] J. H. Kim, A. Y. Jo, Y. J. Choi, K. B. Lee, J. S. Im, and B. C. Bai, "Improving the mechanical strength of carbon–carbon composites by oxidative stabilization," *Journal of Materials Research and Technology*, vol. 9, no. 6, pp. 16513-16521, 2020, https://doi.org/10.1016/j.jmrt.2020.11.064.

[30] R. Guo *et al*., "Polyphenylene sulfide hydrophobic composite coating with high stability, corrosion resistance and antifouling performance," *Surfaces and Interfaces*, vol. 27, p. 101577, 2021, https://doi.org/10.1016/j.surfin.2021.101577.

[31] H. Zheng *et al*., "A durable superhydrophobic polyphenylene sulfide composite coating with high corrosion resistance and good self-cleaning ability," *Colloids and Surfaces A: Physicochemical and Engineering Aspects*, vol. 660, p. 130856, 2023, https://doi.org/10.1016/j.colsurfa.2022.130856.

[32] Y. Seki, E. Kizilkan, B. M. Leşkeri, M. Sarikanat, L. Altay, and A. Isbilir, "Comparison of the Thermal and Mechanical Properties of Poly (phenylene sulfide) and Poly (phenylene sulfide)-Syndiotactic Polystyrene-Based Thermal Conductive Composites," *ACS Omega*, vol. 7, no. 49, pp. 45518–45526, 2022, https://doi.org/10.1021/acsomega.2c06152.

[33] Y. Gao, X. Zhou, M. Zhang, L. Lyu, and Z. Li, "Polyphenylene Sulfide-Based Membranes: Recent Progress and Future Perspectives," *Membranes*, vol. 12, no. 10, p. 924, 2022, https://doi.org/10.3390/membranes12100924.

[34] Y. M. Ghugal, A. S. Sayyad, and S. M. Girme, "Thermoelastic bending analysis of laminated composite shells using a trigonometric shear and normal deformation theory," *Journal of Thermal Stresses*, vol. 45, no. 3, pp. 171-190, 2022, https://doi.org/10.1080/01495739.2022.2030836.

[35] Y. Chen, T. Ye, G. Jin, H. P. Lee, and X. Ma, "A unified quasi-three-dimensional solution for vibration analysis of rotating pre-twisted laminated composite shell panels," *Composite Structures*, vol. 282, p. 115072, 2022, https://doi.org/10.1016/j.compstruct.2021.115072.

[36] M. Meskini and A. R. Ghasemi, "Free vibration analysis of laminated cylindrical adhesive joints with conical composite shell adherends," *Journal of Vibration and Control*, vol. 29, no. 15–16, pp. 3475-3491, 2023, https://doi.org/10.1177/10775463221097466.

[37] A. Melaibari *et al*., "Free Vibration of FG-CNTRCs Nano-Plates/Shells with Temperature-Dependent Properties," *Mathematics*, vol. 10, no. 4, p. 583, 2022, https://doi.org/10.3390/math10040583.

[38] K. Kim, Y. Jon, K. An, S. Kwak, and Y. Han, "A solution method for free vibration analysis of coupled laminated composite elliptical-cylindrical-elliptical shell with elastic boundary conditions," *Journal of Ocean Engineering and Science*, vol. 7, no. 2, pp. 112-130, 2022, https://doi.org/10.1016/j.joes.2021.07.005.

[39] V. Parmar, N. ur Rahman, N. Alam, V. Sharma, and A. Alam, "Finite Element Modelling for Bending and Vibration Analysis of Composite and Sandwich Spherical Shells," *IOP Conference Series: Materials Science and Engineering*, vol. 1225, no. 1, p. 012037, 2022, https://doi.org/10.1088/1757-899X/1225/1/012037.

[40] G. F. O. Ferreira, J. H. S. Almeida, M. L. Ribeiro, A. J. M. Ferreira, and V. Tita, "A finite element unified formulation for composite laminates in bending considering progressive damage," *Thin-Walled Structures*, vol. 172, p. 108864, 2022, https://doi.org/10.1016/j.tws.2021.108864.

[41] Y. Wu, C. Zhao, H. Liang, S. Yao, J. Xue, and P. Xu, "Free vibration of composite cylindrical shells with orthogonal stiffeners," *Journal of Theoretical and Applied Mechanics*, vol. 60, no. 2, pp. 239-252, 2022, https://doi.org/10.15632/jtam-pl/146786.

[42] A. Schiller and C. Bisagni, "Buckling of Composite Cylindrical Shells with Circular Cutouts," *AIAA Science and Technology Forum and Exposition*, 2022, https://doi.org/10.2514/6.2022-1492.

[43] G. Chen, A. K. Mohanty, and M. Misra, "Progress in research and applications of Polyphenylene Sulfide blends and composites with carbons," *Composites Part B: Engineering*, vol. 209, p. 108553, 2021, https://doi.org/10.1016/j.compositesb.2020.108553.

[44] K. Stoeffler, S. Andjelic, N. Legros, J. Roberge, and S. B. Schougaard, "Polyphenylene sulfide (PPS) composites reinforced with recycled carbon fiber," *Composites Science and Technology*, vol. 84, pp. 65-71, 2013, https://doi.org/10.1016/j.compscitech.2013.05.005.

[45] J. S. Won, M. Kwon, J. E. Lee, J. M. Lee, T. J. Kwak, and S. G. Lee, "Polyphenylene sulfide-modified carbon fiber reinforced high-strength composites via electrophoretic deposition," *Journal of Science: Advanced Materials and Devices*, vol. 7, no. 3, p. 100456, 2022, https://doi.org/10.1016/j.jsamd.2022.100456.

[46] K. Zhang, G. Zhang, B. Liu, X. Wang, S. Long, and J. Yang, "Effect of aminated polyphenylene sulfide on the mechanical properties of short carbon fiber reinforced polyphenylene sulfide composites,"

Composites Science and Technology, vol. 98, pp. 57-63, 2014, https://doi.org/10.1016/j.compscitech.2014.04.020.

[47] B. U. Durmaz and A. Aytac, "Characterization of carbon fiber-reinforced poly (phenylene sulfide) composites prepared with various compatibilizers," *Journal of Composite Materials*, vol. 54, no. 1, pp. 89-100, 2020, https://doi.org/10.1177/0021998319859063.

[48] C. S. Kang, H. K. Shin, Y. S. Chung, M. K. Seo, and B. K. Choi, "Manufacturing of Carbon Fibers/Polyphenylene Sulfide Composites via Induction-Heating Molding: Morphology, Mechanical Properties, and Flammability," *Polymers*, vol. 14, no. 21, p. 4587, 2022, https://doi.org/10.3390/polym14214587.

[49] W. Q. Chen and K. Y. Lee, "Benchmark solution of angle-ply piezoelectric-laminated cylindrical panels in cylindrical bending with weak interfaces," *Archive of Applied Mechanics*, vol. 74, no. 7, pp. 466–476, 2005, https://doi.org/10.1007/s00419-004-0357-2.

[50] E. Ameri, M. M. Aghdam, and M. Shakeri, "Global optimization of laminated cylindrical panels based on fundamental natural frequency," *Composite Structures*, vol. 94, no. 9, pp. 2697-2705, 2012, https://doi.org/10.1016/j.compstruct.2012.04.005.

[51] E. Laporte and P. Tallec, "Numerical Methods in Sensitivity Analysis and Shape Optimization," *Modeling and Simulation in Science, Engineering and Technology*, 2003, https://doi.org/10.1007/978-1-4612-0069-7.

[52] N. M. Nurazzi *et al*., "A review on mechanical performance of hybrid natural fiber polymer composites for structural applications," *Polymers*, vol. 13, no. 13, p. 2170, 2021, https://doi.org/10.3390/polym13132170.

[53] K. M. Subhedar, G. S. Chauhan, B. P. Singh, and S. R. Dhakate, "Effect of fibre orientation on mechanical properties of carbon fibre composites," *Indian Journal of Engineering and Materials Sciences*, vol. 27, no. 6, pp. 1100-1103, 2020, https://doi.org/10.56042/ijems.v27i6.47552.

[54] C. Yu, Z. Wang, G. Liu, L. M. Keer, and Q. J. Wang, "Maximum von Mises Stress and Its Location in Trilayer Materials in Contact," *Journal of Tribology*, vol. 138, no. 4, p. 041402, 2016, https://doi.org/10.1115/1.4032888.

[55] A. Avcu, M. Seyedzavvar, C. Boga, and N. Choupani, "Assessing the safety and reliability of type-3 high-pressure composite tanks: a comprehensive analysis of failure metrics," *Sadhana - Academy Proceedings in Engineering Sciences*, vol. 49, no. 55, 2024, https://doi.org/10.1007/s12046-023-02394-8.

[56] B. Vieille and L. Taleb, "About the influence of temperature and matrix ductility on the behavior of carbon woven-ply PPS or epoxy laminates: Notched and unnotched laminates," *Composites Science and Technology*, vol. 71, no. 7, pp. 998-1007, 2011, https://doi.org/10.1016/j.compscitech.2011.03.006.

[57] D. Shi, D. He, Q. Wang, C. Ma, and H. Shu, "Free vibration analysis of closed moderately thick cross-ply composite laminated cylindrical shell with arbitrary boundary conditions," *Materials*, vol. 13, no. 4, p. 884, 2020, https://doi.org/10.3390/ma13040884.

[58] H. Koruk and K. Y. Sanliturk, "A novel definition for quantification of mode shape complexity," *Journal of Sound and Vibration*, vol. 332, no. 14, pp. 3390-3403, 2013, https://doi.org/10.1016/j.jsv.2013.01.039.